molbank

MDPI

Communication

Synthesis of *N*-*p*-Fluorothiosemicarbazone and of Bis(*N*-*p*-Fluorophenylthiourea): Crystal Structure and Conformational Analysis of *N,N′*-Bis(4-Fluorophenyl) Hydrazine-1,2-Bis(Carbothioamide)

Sirine Salhi [1,2], Dorra Kanzari-Mnallah [1,*], Isabelle Jourdain [2], Michael Knorr [2,*], Carsten Strohmann [3], Jan-Lukas Kirchhoff [3], Hédi Mrabet [1] and Azaiez Ben Akacha [1]

1 Laboratory of Selective Organic and Heterocyclic Synthesis-Biological Activity Evaluation (LR17ES01), University of Tunis El Manar, Tunis 2092, Tunisia; hedi.mrabet@fst.utm.tn (H.M.); azaiez.benakacha@fst.utm.tn (A.B.A.)
2 Institut UTINAM UMR 6213 CNRS, Université de Franche-Comté, 16, Route de Gray, 25030 Besançon, France; isabelle.jourdain@univ-fcomte.fr
3 Anorganische Chemie, Technische Universität Dortmund, Otto-Hahn Straße 6, 44227 Dortmund, Germany; carsten.strohmann@tu-dortmund.de (C.S.); jan-lukas.kirchhoff@tu-dortmund.de (J.-L.K.)
* Correspondence: dorra.kanzari@fst.utm.tn (D.K.-M.); michael.knorr@univ-fcomte.fr (M.K.); Tel.: +33-3-8166-6270 (M.K.)

Abstract: The reaction of the phosphonated hydrazone (2-hydrazineylidenepropyl) diphenylphosphine oxide **1** with *p*-fluorophenyl-isothiocyanate yields as a major product the thiosemicarbazone $Ph_2P(=O)CH_2\{C=N\text{-}NH(C=S)\text{-}N(H)C_6H_4F\}CH_3$ (2-(1-(diphenylphosphoryl)propan-2-ylidene)-*N*-(4-fluorophenyl)hydrazine-1-carbothioamide) **2** along with bis(*N*-*p*-fluorophenylthiourea) **3** as a minor product. The latter compound **3** was isolated as the main product by direct treatment of *p*-$FC_6H_4N=C=S$ with hydrazine in a 2:1 ratio. Both **2** and **3** were characterized by NMR. Furthermore, the molecular structure of **3** was elucidated by an X-ray diffraction study, revealing both intra- and intermolecular secondary interactions. A conformational DFT study, at the B3LYP/6-311 G++ (d, p) level of theory, confirms a good match between the calculated structure and the experimental one.

Keywords: thiourea; thiosemicarbazone; crystal structure; conformational analysis; supramolecular network

Citation: Salhi, S.; Kanzari-Mnallah, D.; Jourdain, I.; Knorr, M.; Strohmann, C.; Kirchhoff, J.-L.; Mrabet, H.; Ben Akacha, A. Synthesis of *N*-*p*-Fluorothiosemicarbazone and of Bis(*N*-*p*-Fluorophenylthiourea): Crystal Structure and Conformational Analysis of *N,N′*-Bis(4-Fluorophenyl) Hydrazine-1,2-Bis(Carbothioamide). *Molbank* **2024**, *2024*, M1926. https://doi.org/10.3390/M1926

Academic Editor: Fawaz Aldabbagh

Received: 25 October 2024
Revised: 21 November 2024
Accepted: 22 November 2024
Published: 28 November 2024

1. Introduction

In some previous papers, we have described the synthesis and conformational analysis of a series of phosphonated hydrazones $Ph_2P(=O)CH_2C(=N\text{-}NH_2)CH_3$ and $[R^1R^2C(CH_2O)_2P(=O)CH_2\text{-}C\{=N\text{-}N(H)R^5\}C(H)R^3R^4]$ bearing a six-membered 1,3,2-dioxaphosphorinane heterocycle, which were obtained by treatment of their respective allene precursors with hydrazines [1–4]. The reactivity of these compounds has been subsequently investigated, for example, with ethylorthoformiate, leading to 4-phosphopyrazoles [5].

Since these hydrazones contain a potentially reactive C=N-N(H)R group, these compounds also appeared as suitable starting materials for nucleophilic addition reaction vis-à-vis reactive unsaturated substrates such as isothiocyanates R-N=C=S to afford β-phosphonated thiosemicarbazones. We were intrigued to explore this route, since thiocarbamates feature both promising biological activities (see selected examples in Figure 1) and have found widespread use since the 1970s as ligands in coordination chemistry [6–9].

We describe here our preliminary finding concerning the reactivity of (2-hydrazineylidenepropyl)diphenylphosphine oxide with *p*-fluorophenylisothiocyanate yielding the targeted thiosemicarbazone $Ph_2P(=O)CH_2\{C=N\text{-}NH(C=S)\text{-}N(H)C_6H_4F\}CH_3$ **2**. During the work-up, we also noticed the formation of a second species in minor amounts, the hitherto

unknown compound bis(*N*-*p*-fluorophenylthiourea) **3**. The topic of this communication is focused on (*i*) the optimized preparation and (*ii*) the spectroscopic and detailed crystallographic characterization of this nitrogen- and sulfur-rich compound, whose molecular structure was also (*iii*) subjected to a theoretical conformational analysis by means of a DFT study.

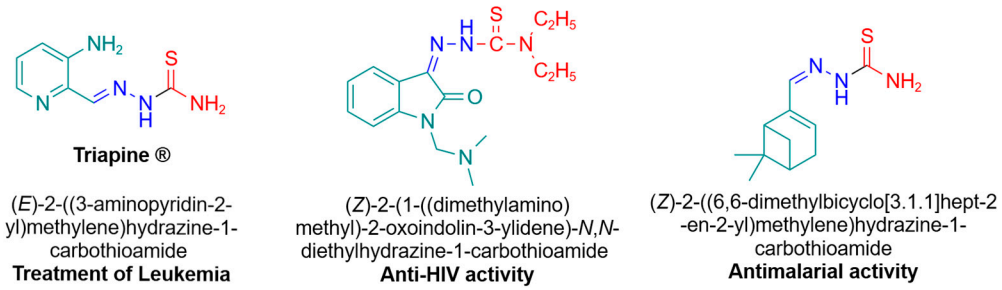

Figure 1. Examples of thiosemicarbazone structures featuring a biological activity [10–12].

2. Results and Discussion

The synthesis of *N*-*p*-fluorothiosemicarbazone **2** is achieved through a condensation reaction of *p*-fluorophenylisothiocyanate with phosphonated hydrazone **1**. The ^{1}H and ^{13}C {^{1}H} NMR spectra of this compound did not show any impurities; even the ^{19}F NMR spectrum contained only the signals of product **2** (Figure S1). However, after crystallization from hot ethanol, a partial decomposition due to cleavage of the $Ph_2P(=O)$ moiety is observed, resulting in the formation of a secondary product, bis(*N*-*p*-fluorophenylthiourea) **3**. Compound **2** displays resonances at about δ 29 ppm in its ^{31}P{^{1}H} NMR spectrum, whereas that of **3** is silent for this nucleus. To fully characterize this new compound, it was synthesized independently via a nucleophilic addition reaction of *p*-fluorophenylisothiocyanate with hydrazine monohydrate (Scheme 1).

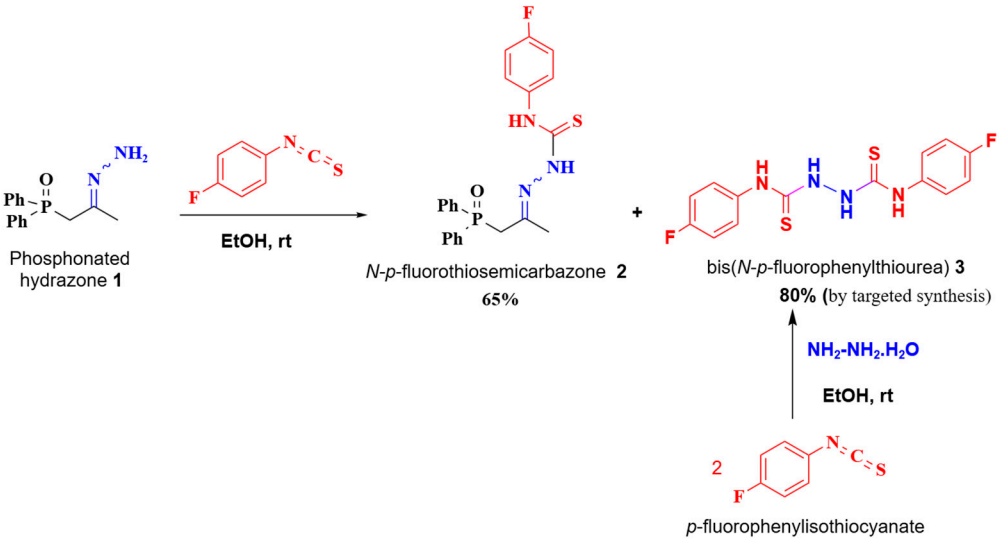

Scheme 1. Synthesis of *N*-*p*-fluorothiosemicarbazone **2** and bis(*N*-*p*-fluorophenylthiourea) **3**. The 80% yield for **3** is obtained upon treatment of hydrazine with 2 equiv. of *p*-fluorophenylisothiocyanate.

The structure of compound **3** was confirmed by NMR, IR spectroscopy and X-ray crystallography. In the IR spectrum of **3**, the strong bands at 3222 and 3074 cm^{-1} are assigned to N-H stretching. The C-N stretching frequency is observed at 1409 cm^{-1}. The thione C=S stretching band appears at 1180 cm^{-1} (Figure S2). This is in good agreement with the characteristic absorption bands observed in the theoretical IR spectrum (Figure S3) and in accordance with the literature [13,14]. The ^{1}H-NMR spectrum recorded in DMSO-d_6 (Figure 2) reveals the aryl signals in the range δ 7.15 to 7.53 ppm. The broad signal at

δ 9.91 ppm can be assigned to the proton of the NH group attached to the phenyl ring, and consequently, the second resonance at δ 9.71 ppm is attributed to the NH group adjacent to the C=S group. The proton-decoupled ^{13}C NMR spectrum (Figure 3) reveals a signal at δ 182.48 ppm, characteristic for a thiocarbonyl group. The doublet appearing at 159.86 ppm is assigned to the carbon C2 due to a strong $^{1}J_{FC}$ coupling of 241 Hz. The remaining peaks observed between 115 and 136 ppm correspond to aromatic carbons, as attributed in Figure 2. Both the ^{1}H and ^{13}C NMR spectra reveal the presence of other signals, and we suppose that they are due to a second conformational isomer in a low equilibrium concentration.

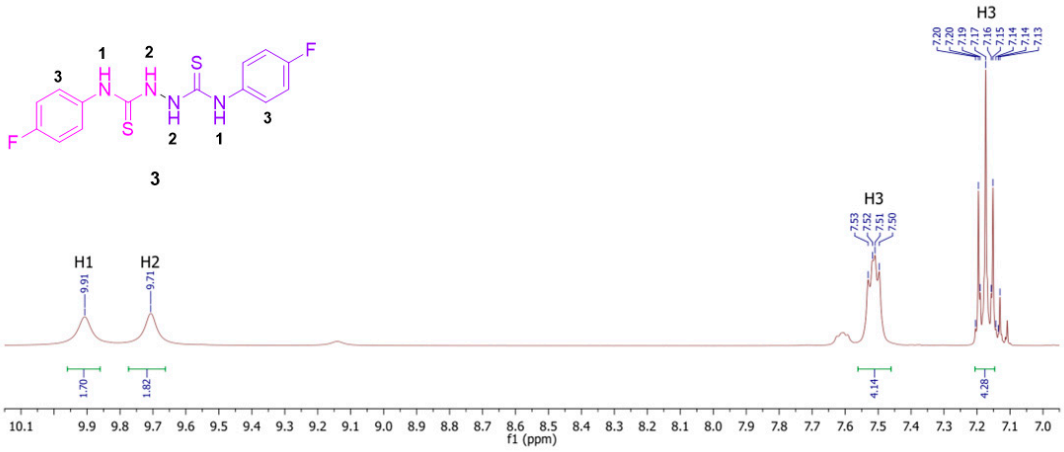

Figure 2. ^{1}H NMR spectrum (400 MHz, DMSO-d_6) of compound **3** at 298 K. The remaining weak resonances indicate the presence of a second conformer of **3** at a low equilibrium concentration.

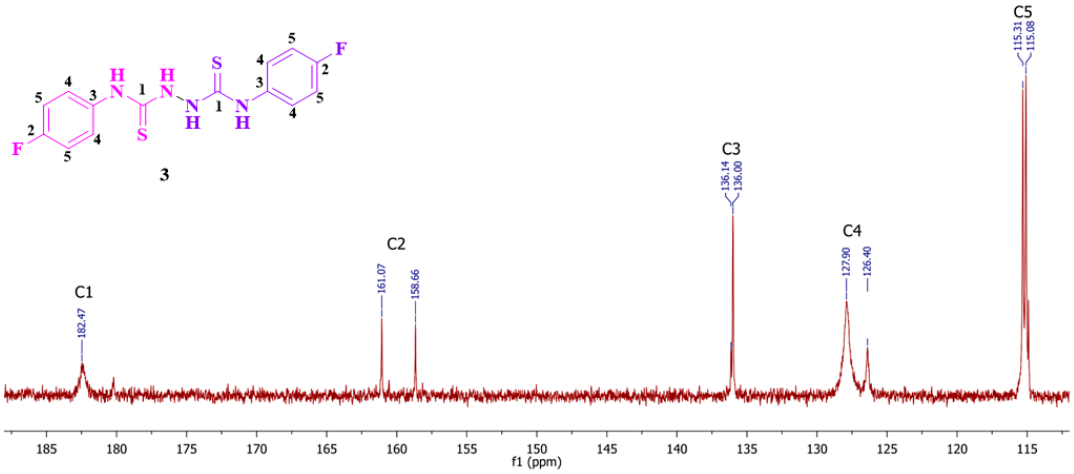

Figure 3. ^{13}C{^{1}H} NMR spectrum (100 MHz, DMSO-d_6) of compound **3** at 298 K. The DMSO-d_6 signal has been cut off.

As shown in Figure 4, a crystallographic investigation of bis(*N*-*p*-fluorophenylthiourea) **3** performed at 100 K shows that the solid-state structure has an inversion center between the two nitrogen atoms N2, with the asymmetric unit displaying only half of compound **3**. This can be explained by the fact that the center of the molecule is located on a two-fold axis. Both the C1–N1 and C1–N2 bonds of 1.332(2) and 1.367(2) Å are shorter than the C2–N1 bond (1.440(2) Å), reflecting a partial double bond character. The torsion angle C1-N2–N2–C1 amounts to −125.52°, so **3** adopts a s-*cis* or *cisoid* conformation similar to that reported in previous studies for related derivatives bearing a phenyl or cyclohexyl cycle (see also below for the conformational analysis) [15,16]. In fact, Akinchan et al. studied bis(*N*-phenylthiourea) and found a s-*cis* conformation of the two thiosemicarbazone moiety (Figure 5a) [15]. A s-*cis* conformation of the thiosemicarbazone moiety was also reported

by Jaiswal et al. [16] for the structure of bis(*N*-cyclohexylthiourea) Figure 5b). However, a *transoid* conformation around the central N–N bond was crystallographically ascertained for *N*,*N*′-bis(benzamidothiocarbonyl)hydrazine (Figure 5c) and for *N*,*N*′-(hydrazine-1,2-diyldicarbonothioyl)bis(2-chlorobenzamide) [17–19]. This *transoid* conformation observed for the latter benzoyl derivatives is probably forced by an intramolecular O···H bonding.

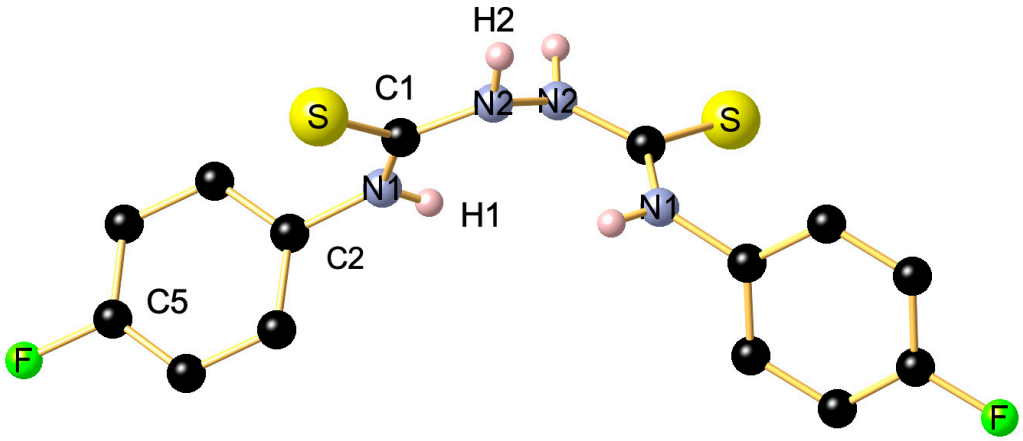

Figure 4. Molecular structure of **3** in the crystal. Selected bond lengths (Å) and angles (°): S1–C1 1.6970 (17), F1–C5 1.366 (2), N2–N2[1] 1.404 (3), N2–C1 1.367 (2), N1–C1 1.332 (2), N1–C2 1.440 (2); C1–N2–N21 119.70 (16), C1–N1–C2 122.29 (14), N2–C1–S1 118.08 (12), N1–C1–N2 118.08 (15), C3–C2–N1 119.35 (16), C7–C2–N1 119.77 (16), F1–C5–C4 118.36 (19), F1–C5–C6 118.33 (19). Symmetry operation to generate equivalent atoms: [1]1-*x*, +*y*, 3/2-*z*.

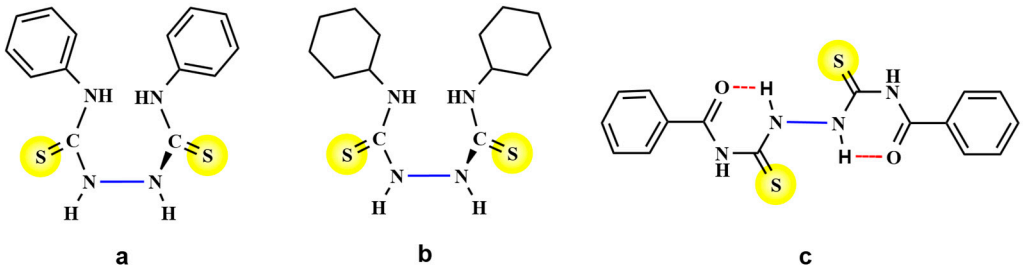

Figure 5. Other examples of crystallographically characterized bis(thioureas) adopting a *cisoid* (**a**,**b**) or a *transoid* conformation (**c**) with respect to the central N–N bond [13,15–17].

All hydrogen atoms from the NH groups are involved in intermolecular hydrogen bonds with sulfur atoms as shown in Figure 6.

Additionally, the inter- and supramolecular interactions of compound **3** were further analyzed using a Hirshfeld analysis. *CrystalExplorer21* was employed to calculate a three-dimensional Hirshfeld surface [20]. The surface is depicted in Figure 7. Particularly significant are the very strong N2–H2···S1 interactions in the solid state, which are prominently observable. The distance between atoms N2 and S1 is 3.2749(16) Å, and the high linear bond angle of 164.4(19)° further confirms the presence of a strong hydrogen bond within the crystal. Moreover, additional interactions can be identified on the Hirshfeld surface. The somewhat weaker N1–H1···S1 interaction, despite having a shorter overall contact of 3.2675(15) Å (N1–S1), exhibits a smaller angle of 141.9(18)°. As a result, the H2···S1 contact is shorter [2.42(2) Å] compared to the longer H1···S1 contact [2.56(2) Å]. Decisive, however, is the significantly more linear angle of the N2–H2···S1 interaction compared to the N1–H1···S1 interaction, which could be primarily responsible for the packing within the crystal structure and shows a correspondingly strong expression on the Hirshfeld surface (see Figure 7).

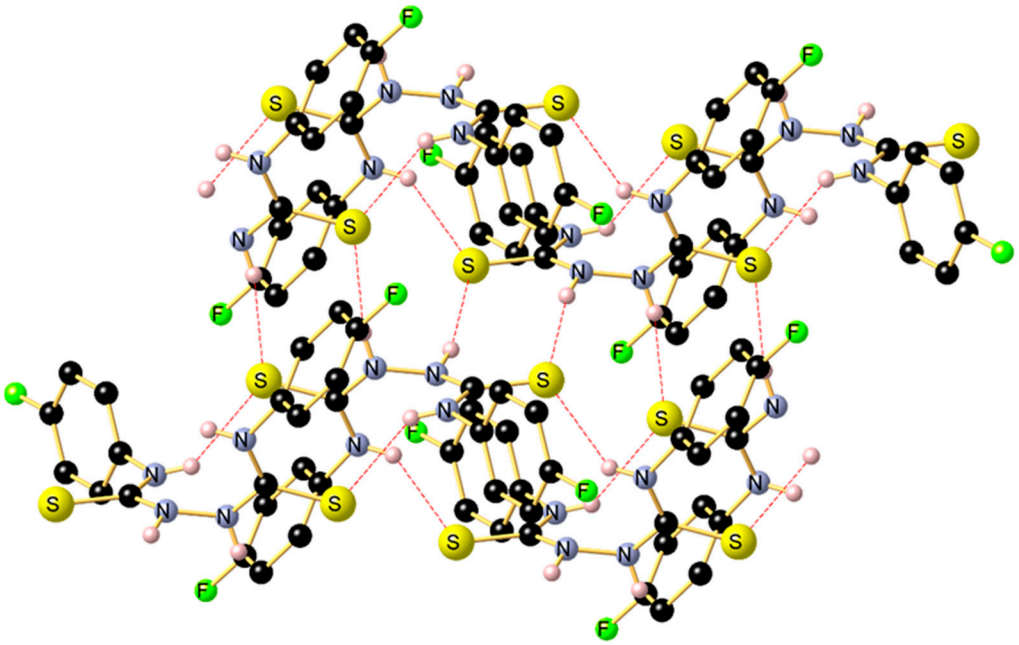

Figure 6. Supramolecular secondary interactions occurring in the crystal structure of **3**.

Other multiple contacts are present here as well, which contribute to the extended supramolecular network. Finally, a weaker C6–H6···F1 interaction is observed, characterized by a separation of 3.291(2) Å (C6–F1) and an angle of 135.8(18)°. This indicates that, due to the lower degree of linearity, this interaction is relatively weak. The analysis of the fingerprint plots, whose illustrations can be found in the Supporting Information (Figure S4), also suggests that the S···H contacts are particularly pronounced and reflect the most significant supramolecular interactions. Table 1 summarizes all relevant hydrogen bonds in the solid-state structure.

Table 1. Selected hydrogen bonds of compound **3** between the donor atom (D) and the acceptor atom (A); the distances $d_{D–H}$, $d_{H–A}$, $d_{D–A}$ as well as the angle D–H–A are listed.

D	H	A	$d_{D–H}$/Å	$d_{H–A}$/Å	$d_{D–A}$/Å	D–H–A/°
N2	H2	S1	0.88(2)	2.42(2)	3.2749(16)	164.4(19)
N1	H1	S1	0.85(2)	2.56(2)	3.2675(15)	141.9(18)
C6	H6	F1	0.94(2)	2.55(2)	3.291(2)	135.8(18)
C7	H7	F1	0.96(2)	3.08(2)	3.684(2	122.6(15)

In addition to hydrogen bonding, the crystal structure of **3** was examined for π–π interactions. Figure 6 already shows that the packing within the cell is so arranged that the aromatic ring systems are stacked on top of each other. To determine the exact distance and significance of these interactions, the centroid of a symmetry-generated aromatic ring C2–C7 (1 -*x*, +*y*, 3/2 -*z*) was calculated and repeated for the neighboring aromatic ring. The analysis of the centroid-to-centroid distance revealed a separation of 4.8775(6) Å and a ring-to-ring angle of 138.62(9)°. These values indicate that π–π interactions are weak in compound **3**, though they may contribute to the stabilization of the packing.

To optimize the electronic structure of bis (*N*-*p*-fluorophenylthiourea) **3**, a theoretical study DFT calculation using the B3LYP/ 6-311++ G (d, p) basis set was performed both in the gas and various solvent (ethanol/methanol/chloroform/acetonitrile) phases with varying polarities. The optimized molecular geometry of **3** adopting a s-*cis* or *cisoid* conformation of the thiosemicarbazone moiety is reported in Figure 8.

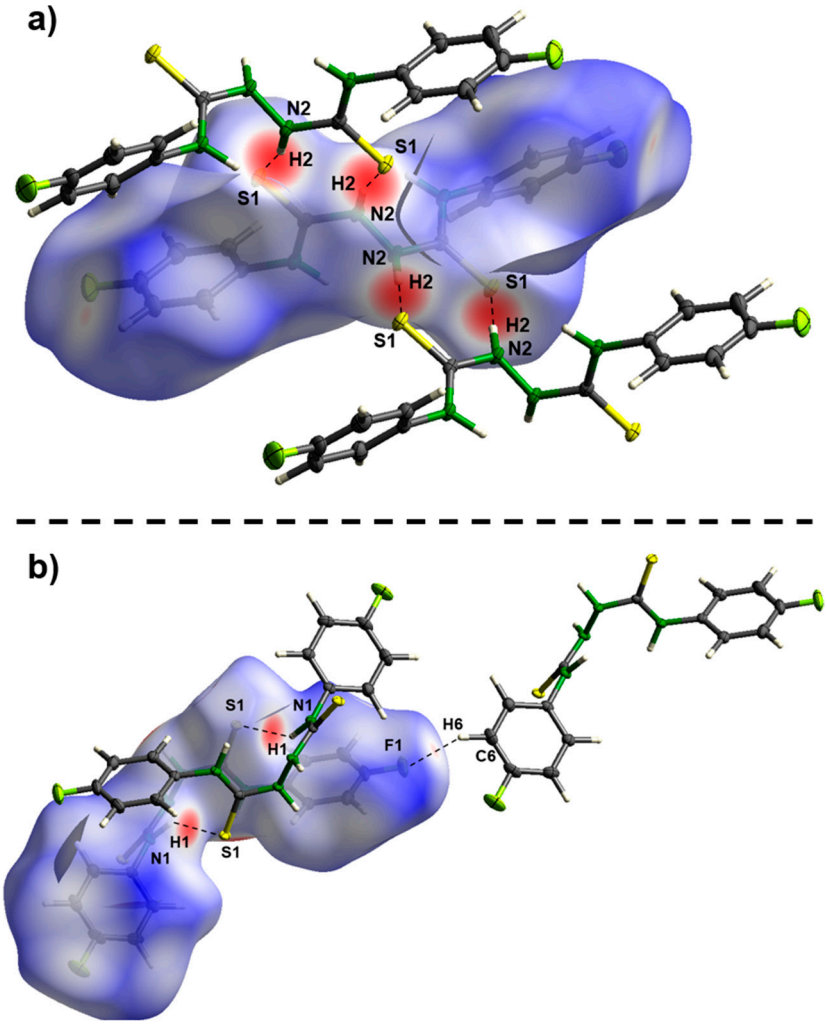

Figure 7. Hirshfeld surface of compound **3** (–0.4235 to 1.5420 arbitrary units): (**a**) visualization of the very strong N2–H2···S1 interactions with two other molecules in the solid state; (**b**) representation of the strong N1–H1···S1 interactions with another molecule in the solid state, as well as weak C6–H6···F1 interactions in the solid state of compound **3**.

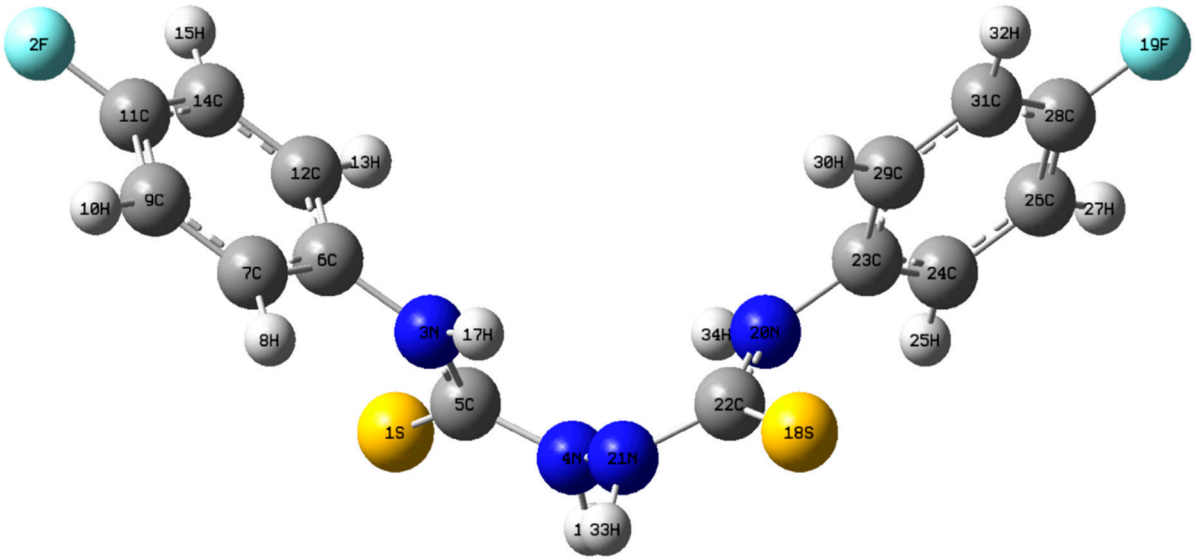

Figure 8. Optimized structure of **3** using DFT/ B3LYP/6-311++ G (d,p).

A comparison of selected geometrical parameters of the DFT-optimized structures in solvent with the experimental structure obtained by SCXRD was investigated. The essential bond lengths and angle values are shown in Table 2. The best matches were obtained using ethanol and methanol as the solvent model, whereas the gas-phase data were less satisfying (Table S6). Representative torsion angles are given in the Supplementary Materials as Table S7. It can be observed that calculated bond lengths are close to the experimental ones. The slight difference between the SCXRD- and DFT-calculated angles is certainly due to the fact that the X-ray crystallographic data were collected from the crystal lattice of complex molecules interacting with the neighboring ones. Therefore, the presence of the intermolecular interactions, described above and illustrated in Figure 6, cannot be taken in account in the computational study. The calculated S1-C5 bond of 1.684 Å in ethanol, methanol and acetonitrile is similar to the experimental value of 1.697(17) Å, revealing a double bond character (Table 2). These values match again with those reported in the literature [15,16]. For example, Akinchan et al. [15] experimentally found the bond length of S1-C5 in the bis(*N*-phenylthiourea) (Figure 5a) equal to 1.681(3) Å. Jaiswal et al. reported experimental and calculated values (using DFT, B3LYP, 6-311 ++ G (d, p), in the gaseous phase) of 1.695(3) and 1.696 Å for the S1-C5 bond in bis(*N*-cyclohexylthiourea) (Figure 5b) [16]. Identical calculated bond lengths were found for N4-N21: 1.392 Å in ethanol, methanol and acetonitrile phases corresponding to 1.404(3) Å in SC-XRD. A comparison of the parameters calculated for the four solvents studied reveals that chloroform, having the least polarity, deviates furthest from the SC-XRD parameter values. The calculated C5-N4-N21-C22 torsion angle of −119.95° in ethanol phase corresponds to the experimental value of −125.65°, with a deviation of 5.7 Å, indicating a skew conformation of the molecule (Table S7). A similar conformation was crystallographically found for bis(*N*-phenylthiourea) (Figure 5a), with a C5-N4-N21-C22 torsion angle of −121.8(3)° [15].

Table 2. Selected bond lengths (Å) and angles (°) for **3** from X-ray diffraction and DFT optimization *.

Bond Lengths (Å)	Exp SCXRD	Calc. in EtOH **	Calc. in MeOH	Calc. in MeCN	Calc. in $CHCl_3$	Angles (°)	Exp. SCXRD	Calc. in EtOH	Calc. in MeOH	Calc. in MeCN	Calc. in $CHCl_3$
S1-C5	1.697(17)	1.684	1.684	1.684	1.678	C5-N4-N21	119.70(16)	120.84	120.84	120.84	121.09
F2-C11	1.366(2)	1.361	1.361	1.361	1.358	C5-N3-C6	122.29(14)	127.48	127.46	127.45	127.61
N4-N21	1.404(3)	1.392	1.392	1.392	1.390	N4-C5-S1	118.08(12)	118.46	118.45	118.46	118.46
N4-C5	1.367(2)	1.388	1.387	1.387	1.390	N3-C5-S1	123.81(13)	126.85	126.81	126.81	127.11
N3-C5	1.332(2)	1.343	1.343	1.343	1.346	C7-C6-N3	119.35(16)	118.59	120.07	121.07	118.41
N3-C6	1.440(2)	1.426	1.426	1.426	1.427	N3-C5-N4	118.08(15)	114.68	114.71	114.72	114.38
C6-C7	1.394(2)	1.395	1.396	1.396	1.395	F2-C11-C9	118.36(19)	118.71	118.64	118.64	118.74

* The atom numbering is shown in the optimized structure of **3**. ** Descending order of polarity of the tested solvents: MeOH (ε = 32.6) > EtOH (ε = 24.3) > MeCN (ε = 36.0) > $CHCl_3$ (ε = 4.81).

3. Materials and Methods

All reagents were obtained from commercial suppliers and used without further purification. ^{1}H and $^{13}C\{^{1}H\}$ NMR spectra were acquired using a Bruker AC 400 spectrometer (Bruker, Wissembourg, France) operating at 400 MHz and 100 MHz, respectively. The infrared spectrum was recorded in ATR mode using a Vertex 70 spectrometer (Bruker, Wissembourg, France).

***Synthesis of compound* 2:** *p*-fluorophenyl-isothiocyanate (0.01 mol, 1.53 g) was added dropwise to a solution of β-phosphonate hydrazone 1 (0.01 mol, 2.72 g) and absolute ethanol (25 mL). The reaction mixture was stirred at room temperature until the formation of white precipitate. Yield = 2.75 g, 65%, $C_{22}H_{21}FN_3OPS$ (M.W. = 425.46 g. mol^{-1}) white solid, mp (°C ±2): 198. *Z*-isomer: $^{31}P\{^{1}H\}$ NMR (DMSO-d_6) at 298 K: 28.94. ^{19}F NMR (DMSO-d_6) at 298 K: −117.41. ^{1}H NMR (DMSO-d_6) at 298 K: 1.81 (d, $^{4}J_{HP}$ 2.2 Hz, 3H, CH_3), 4.01 (d, $^{2}J_{HP}$ 15.55 Hz, 2H, CH_2-P), 7.14–7.94 (m, H_{arom}), 9.84 (s, 1H, N-NH), 11.16 (s, 1H,

NH-*p*-F-Ph). $^{13}C\{^1H\}$ NMR (DMSO-d_6) at 298 K: 25.82 (d, $^3J_{CP}$ 2.51 Hz, CH_3), 126.85–136.00 (m, C_{arom}), 146.54 (d, $^2J_{CP}$ 9.08 Hz, C=N), 159.91 (d, $^1J_{CF}$ 241.8 Hz, C-F), 177.59 (s, C=S). *E*-isomer: $^{31}P\{^1H\}$ NMR (DMSO-d_6) at 298 K: s, 26.97. ^{19}F NMR (DMSO-d_6) at 298 K: −117.33. ^1H NMR (DMSO-d_6) at 298 K: 2.01 (d, $^4J_{HP}$ 1.35 Hz 3H, CH_3), 3.73 (d, $^2J_{HP}$ 13.4 Hz, 2H, CH_2-P), 7.14–7.94 (m, H_{arom}), 9.63 (s, 1H, N-NH), 10.72 (s, 1H, NH-*p*-F-Ph). $^{13}C\{^1H\}$ NMR (DMSO-d_6) at 298 K: 19.01 (d, $^3J_{CP}$ 2.51 Hz, CH_3), 34.61 (d, $^1J_{CP}$ = 61.69 Hz, CH_2-P), 126.85–136.00 (m, C_{arom}), 147.89 (d, $^2J_{CP}$ 8.9 Hz, C=N), 159.83 (d, $^1J_{CF}$ = 241.9 Hz, C-F), 176.89 (s, C=S).

***Synthesis of compound* 3:** *p*-fluorophenyl isothiocyanate (0.01 mol, 1.53 g) was dissolved in 25 mL of ethanol. To this solution, hydrazine monohydrate (0.005 mol, 0.25 g) was added dropwise. The resulting mixture was then stirred at room temperature for 2 h. The precipitate was filtered and washed with ice-cold ethanol and crystalized from hot ethanol. Yield: (1.35 g, 80%). $C_{14}H_{12}F_2N_4S_2$ (M.W. = 338.39 g.mol^{-1}) white solid, mp > 225 °C, IR-ATR: 3074 ν(NH), 1180 ν(C=S) cm^{-1}. ^{19}F NMR (DMSO-d_6) at 298 K: −117.48. ^1H NMR (DMSO-d_6) at 298 K: δ 7.15–7.53 (m, H_{arom}), 9.71 (s, HN-C=S), 9.91 (s, HN-Ar) ppm. $^{13}C\{^1H\}$ NMR (DMSO-d_6) at 298 K: δ 115.19 (C5), 127.15 (C4), 136.00 (C3), 159.86 (d, $^1J_{CF}$ 242.1 Hz, C2), 182.48 (C1) ppm.

The crystallographic data collection was performed on a Bruker D8 Venture four-circle diffractometer from Bruker AXS GmbH (Karlsruhe, Germany). A Photon II from Bruker AXS GmbH was used as a CPAD detector, and the X-ray sources were a Microfocus source IμS Mo from Incoatec GmbH with HELIOS mirror optics and a single-hole collimator from Bruker AXS GmbH. Programs used for data collection were APEX4 Suite [21] (v2021.10-0) and integrated programs SAINT (V8.40A; integration as well as SADABS (2018/7; absorption correction) from Bruker AXS GmbH [21]. The SHELX programs were used for further processing [22]. The solution of the crystal structures was performed with the help of the program SHELXT [23] and the structure refinement with SHELXL [24]. The processing and finalization of the crystal structure data were carried out with program OLEX2 v1.5 [25]. All non-hydrogen atoms were refined anisotropically. All H atoms were refined freely using independent values for each U_{iso}(H).

Crystal data for $C_{14}H_{12}F_2N_4S_2$: M = 338.39 g·mol^{-1}, white crystals, crystal size 0.231 × 0.147 × 0.032 mm^3, monoclinic, space group *C2*/c *a* = 26.6377 (17) Å, *b* = 6.4831 (4) Å, *c* = 9.2178 (6) Å, α = 90°, β = 96.244 (3)°, γ = 90°, *V* = 1582.42 (17) Å^3, *Z* = 4, D_{calc} = 1.420 g/cm^3, *T* = 100 K, R_1 = 0.0600, Rw_2 = 0.0785 (all data) for 12604 reflections with I > = 2σ (I) and 2051 independent reflections, GOF = 1.058 Largest diff. peak/hole/e Å^{-3} 0.27/−0.27.

Data were collected using graphite monochromated MoK_α radiation λ = 0.71073 Å and have been deposited at the Cambridge Crystallographic Data Centre as CCDC 2382121. (Supplementary Materials). The data can be obtained free of charge from the Cambridge Crystallographic Data Centre via http://www.ccdc.cam.ac.uk/getstructures (accessed on 19 November 2024).

Theoretical Calculations

All computations were performed with the Gaussian 09 program [26,27]. The conformation was optimized using DFT geometry optimizations using hybrid B3LYP [28] functional and the 6-311++ G (d, p) basis set. To be sure that all optimized structure lay at a local point on the potential energy surface, harmonic vibrational frequencies of all structures were analyzed. None of the predicted spectra has any imaginary frequencies.

4. Conclusions

We have demonstrated that the *N*-*p*-fluorothiosemicarbazone $Ph_2P(=O)CH_2\{C=N\text{-}NH(C=S)\text{-}N(H)C_6H_4F\}CH_3$ **2** is readily accessible as the main product by treatment of hydrazone $Ph_2P(=O)CH_2C(=N\text{-}NH_2)CH_3$ **1** with *p*-fluorophenyl-isothiocyanate. As a side product, the formation of minor amounts of bis(*N*-*p*-fluorophenylthiourea) **3** was also evidenced, which alternatively have been synthesized in a targeted manner by direct addition of hydrazine hydrate to *p*-fluorophenylisothiocyanate. For the latter compound,

whose crystal structure reveals both intra- and intermolecular secondary interactions, a conformational analysis was also performed by means of DFT computing. We are currently investigating whether treatment of 1 with other aryl- and alkylisothiocyanates constitutes a general synthetic access to thiosemicarbazone and are analyzing conformational aspects in more detail. We are furthermore probing their potential as functionalized *S*,*N* chelate ligands in coordination chemistry.

Supplementary Materials: The following supporting information can be downloaded, ^{1}H NMR spectrum of compound **2**, CIF file, Check-CIF report, Hirshfeld fingerprint plots, IR spectra.

Author Contributions: S.S. prepared the compounds, and D.K.-M. performed the conformational analysis; C.S. and J.-L.K. collected the X-ray data and determined the structure; I.J., D.K.-M. and M.K. designed the study, analyzed the data and wrote the paper. A.B.A., I.J., D.K.-M., H.M. and M.K. contributed to the conceptualization. All authors have read and agreed to the published version of the manuscript.

Funding: This work has been achieved in the frame of the EIPHI Graduate school (contract "ANR-17-EURE-0002").

Data Availability Statement: The X-ray data are at CCDC as stated in the paper.

Acknowledgments: We thank Stéphanie Beffy for recording the IR and NMR spectra. C.S. and J.-L.K. thank the *Fonds der Chemischen Industrie* and the *Konrad-Adenauer-Stiftung* for financial support.

Conflicts of Interest: The authors declare no conflicts of interest.

References

1. Kanzari-Mnallah, D.; Salhi, S.; Knorr, M.; Kirchhoff, J.L.; Strohmann, C.; Efrit, M.L.; Akacha, A.B. Synthesis of Isomeric β-Cycloalkoxyphosphonated Hydrazones Containing a Dioxaphosphorinane Ring: Conformational and Conformational Investigation and Molecular Docking Analysis. *J. Mol. Struct.* **2024**, *1317*, 139035. [CrossRef]
2. Ben Akacha, A.; Barkallah, S.; Zantour, H. ^{13}C NMR and ^{31}P NMR Spectral Assignment of New β-Phosphonylated Hydrazones. *Magn. Reson. Chem.* **1999**, *37*, 916–920. [CrossRef]
3. Kanzari-Mnallah, D.; Efrit, M.L.; Ben Akacha, A. Synthèse de 1,3,2-Dioxaphosphorinanes Diastéréoisomères: Influence de la Conformation des 1,3-Diols de Départ sur Leurs Structures et Conformations. *Phosphorus Sulfur Silicon Relat. Elem.* **2017**, *192*, 665–673. [CrossRef]
4. Salah, N.; Arfaoui, Y.; Bahri, M.; Efrit, M.L.; Ben Akacha, A. Synthèse et Étude Conformationnelle par RMN (^{1}H, ^{13}C, ^{31}P) et DFT des Cycloalcoxyphosphinallenes et des Hydrazones β-Cycloalcoxyphosphonatées. *Phosphorus Sulfur Silicon Relat. Elem.* **2013**, *188*, 609–622. [CrossRef]
5. Ben Akacha, A.; Ayed, N.; Baccar, B.; Charrier, C. Phospho-4-Pyrazoles. Synthesis and Proton, Phosphorus-31, and Carbon-13 NMR. *Phosphorus Sulfur Relat. Elem.* **1988**, *40*, 63–68. [CrossRef]
6. Nurkenov, O.A.; Ibrayev, M.K.; Satpaeva Zh, B.; Dauletzhanova Zh, T.; Seilkhanov, T.M. Synthesis and Study of Antioxidant Activity of Hydrazone and Thiosemicarbazide Based on *N*-Morpholinoacetic Acid Hydrazide. *Vestnik Karaganda Univ. Ser. Chem.* **2018**, *1*, 22–26. [CrossRef]
7. Gihsoyl, A.; Terzioglu, N.; Bik, G. Synthesis of Some New Hydrazide-Hydrazones, Thiosemicarbazides, and Thiazolidinones as Possible Antimicrobials. *Eur. J. Med. Chem.* **1997**, *32*, 753–757. [CrossRef]
8. Salah, N.; Zribi, S.; Efrit, M.L.; Ben Akacha, A. Hydrazones β-Phosphonates: Nouvelles Voies d'Accès aux Thiosemicarbazones, 4-Phosphopyrazoles et Indoles 2-Phosphonates. *J. Soc. Chim. Tunisie* **2013**, *15*, 133–141.
9. Ragab, A.; Ammar, Y.A.; Mahmoud, M.; Mohamed, B.I.; El-Tabl, S.; Abdou; Farag, S.S. Synthesis, Characterization, Thermal Properties, Antimicrobial Evaluation, ADMET Study, and Molecular Docking Simulation of New Mono Cu (II) and Zn (II) Complexes with 2-Oxoindole Derivatives. *Comput. Biol. Med.* **2022**, *145*, 105473. [CrossRef]
10. Dharmasivam, M.; Kaya, B.; Wijesinghe, T.; Azad, M.G.; Gonzálvez, M.A.; Hussaini, M.; Chekmarev, J.; Bernhardt, P.V.; Richardson, D.R. Designing Tailored Thiosemicarbazones with Bespoke Properties: The Styrene Moiety Imparts Potent Activity, Inhibits Heme Center Oxidation, and Results in a Novel "Stealth Zinc (II) Complex". *J. Med. Chem.* **2023**, *66*, 1426–1453. [CrossRef]
11. Bal, T.R.; Anand, B.; Yogeeswari, P.; Sriram, D. Synthesis and Evaluation of Anti-HIV Activity of Isatin β-Thiosemicarbazone Derivatives. *Bioorg. Med. Chem. Lett.* **2005**, *15*, 4451–4455. [CrossRef] [PubMed]
12. De Oliveira, R.B.; de Souza-Fagundes, E.M.; Soares, R.P.P.; Andrade, A.A.; Krettli, A.U.; Zani, C.L. Synthesis and Antimalarial Activity of Semicarbazone and Thiosemicarbazone Derivatives. *Eur. J. Med. Chem.* **2008**, *43*, 1983–1988. [CrossRef] [PubMed]
13. Firdausiah, S.; Hasbullah, S.A.; Yamin, B.M. Synthesis, Structural Elucidation, and Antioxidant Study of Ortho-Substituted *N*, *N*′-bis(benzamidothiocarbonyl)hydrazine Derivatives. *J. Phys. Conf. Ser.* **2018**, *979*, 012010. [CrossRef]
14. Mészáros Szécsényi, K.; Leovac, V.M.; Radosavljević Evans, I. Synthesis and Characterisation of a Novel Polymeric Cd Complex, Catena-(μ-Thio)[bis(N-Phenylthiourea)] bis(dimethylsulfoxide)dichlorocadmium (II). *J. Coord. Chem.* **2006**, *59*, 171–180. [CrossRef]

15. Akinchan, N.T.; Drożdżewski, P.M.; Battaglia, L.P. Crystal structure and spectroscopic characterization of bis(*N*-phenylthiourea). *J. Chem. Crystallogr.* **2002**, *32*, 91–97. [CrossRef]
16. Jaiswal, S.; Gond, M.K.; Bharty, M.K.; Maiti, B.; Krishnamoorthi, S.; Butcher, R.J. Manganese (II) catalyzed synthesis of bis (N-cyclohexylthiourea) derived from thiosemicarbazide: Structural characterization, fluorescence, cyclic voltammetry, Hirshfeld surface analysis and DFT calculation. *J. Mol. Struct.* **2021**, *1246*, 131060–131070. [CrossRef]
17. Yamin, B.M.Y.; Yusof, M.S.M. N,N′-Bis(benzamidothiocarbonyl)hydrazine Dimethyl Sulfoxide Disolvate. *Acta Crystallogr. Sect. E Struct. Rep. Online* **2003**, *59*, o358–o359. [CrossRef]
18. Deepthi, S.; Rajalakshmi, K.; Gunasekaran, K.; Velmurugan, D.; Nagarajan, K. Crystal and Molecular Structure of Addition Products of Dimethyl Acetylene Dicarboxylate and *N*,*N*′- Thiocarbanilyl Hydrazine. *Mol. Cryst. Liq. Cryst.* **2001**, *369*, 221–343. [CrossRef]
19. Both preparation of bis(*N*-p-chlorophenylthiourea and bis(*N*-p-methoxyphenylthiourea have been reported, but these deriva-tives are not crystallographically characterized: Herrero, J.M.; Fabra, D.; Matesanz, A.I.; Hernández, C.; Sánchez-Pérez, I.; Quiroga, A.G. Dithiobiureas Palladium (II) Complexes' Studies: From Their Synthesis to Their Biological Action. *J. Inorg. Biochem.* **2023**, *246*, 112261. [CrossRef]
20. Spackman, P.R.; Turner, M.J.; McKinnon, J.J.; Wolff, S.K.; Grimwood, D.J.; Jayatilaka, D.; Spackman, M.A. CrystalExplorer: A Program for Hirshfeld Surface Analysis, Visualization, and Quantitative Analysis of Molecular Crystals. *J. Appl. Cryst.* **2021**, *54*, 1006–1011. [CrossRef]
21. Bruker. *Apex 4*; Bruker AXS Inc.: Madison, WI, USA, 2021.
22. Sheldrick, G.M. A Short History of SHELX. *Acta Cryst. A* **2008**, *64*, 112–122. [CrossRef] [PubMed]
23. Sheldrick, G.M. SHELXT—Integrated Space-Group and Crystal-Structure Determination. *Acta Cryst. A* **2015**, *71*, 3–8. [CrossRef] [PubMed]
24. Sheldrick, G.M. Crystal Structure Refinement with SHELXL. *Acta Cryst. C* **2015**, *71*, 3–8. [CrossRef] [PubMed]
25. Dolomanov, O.V.; Bourhis, L.J.; Gildea, R.J.; Howard, J.A.K.; Puschmann, H. OLEX2: A Complete Structure Solution, Refinement and Analysis Program. *J. Appl. Cryst.* **2009**, *42*, 339–341. [CrossRef]
26. Frisch, M.J.; Trucks, G.W.; Schlegel, H.B.; Scuseria, G.E.; Robb, M.A.; Cheeseman, J.R.; Scalmani, G.; Barone, V.; Mennucci, B.; Petersson, G.A.; et al. *Gaussian 09: Revision A.1*; Gaussian Inc.: Wallingford, CT, USA, 2009.
27. Dennington, R.D.; Keith, T.A.; Millam, J.M. *GaussView 5.0.8*; Gaussian Inc.: Wallingford, CT, USA, 2008.
28. Becke, A.D. Density functional thermochemistry. III. The role of exact exchange. *J. Chem. Phys.* **1993**, *98*, 1372–1377. [CrossRef]